VISIBLE-LIGHT-ACTIVE NITROGEN DOPED TiO_2 NANOPARTICLES PREPARED BY SOL-GEL ACID CATALYZED REACTION

S. Janitabar Darzi*[,1], A. R. Mahjoub[2] and S. Sarfi[1]

* *sjanitabar@aeoi.org.ir*

Received: January 2012 **Accepted: August 2012**

[1] Nuclear Fuel Cycle Research School, Nuclear Science and Technology Research Institute AEOI, Tehran, Iran.
[2] Faculty of Science, Tarbiat Modares University, 14115-175, Tehran, Iran.

Abstract: *Yellow-colored nitrogen doped TiO_2 photocatalyst and a pure TiO_2 powder were synthesized via sol-gel method using $TiCl_4$ and urea as raw materials. However, the synthesis procedure for nitrogen doped TiO_2 was catalyzed by acid that dialed with controlled precipitation and slow nucleation. According to XRD analysis, the nitrogen doped TiO_2 consisted of anatase phase of titania which was a significant achievement regarding its possible photocatalytic applications. The band gaps of nitrogen doped TiO_2 and pure TiO_2 were estimated from UV-Vis spectroscopy data to be 2.8 and 3.3 ev, respectively. Photocatalytic properties of the nitrogen doped TiO_2 nanocatalyst and pure TiO_2 were compared for degradation of crystal violet dye in visible light irradiation. In comparison to pure TiO_2, nitrogen doped TiO_2 showed superior photocatalytic efficiency towards the dye.*

Keywords*: TiO_2, sol-gel, band gap, nitrogen, nanoparticles.*

1.INTRODUCTION

Titanium dioxide (TiO_2), as a chemically stable, nontoxic, highly efficient, and relatively inexpensive photocatalyst, has been widely used for water and air purification since many environmental pollutants can be degraded by oxidation and reduction processes on TiO_2 surface [1- 3]. However, the TiO_2 photocatalyst has not been applied widely in the field of environmental pollution control, since its large band gap energy (Eg = 3.2 eV) considerably limits the utilization of natural solar light or artificial visible light. Modification of TiO_2 to extend its absorption edge toward the visible light region has been the subject of recent research [4].

TiO_2 was used as visible light photocatalysts by substitution doping of metal ions, ion implantation, organic dye sensitization, and hydroxide or surface coordination. However, these modified photocatalysts, in general, show a weak absorption in the visible light region and deactivate easily.

Band-gap narrowing by the introduction of nonmetal anions (N, C, S and F) into TiO_2 was recently found to be more efficient than the traditional methods to yield catalyst with high catalytic activity under visible light irradiation [5].Theoretical calculations showed that the p-orbitals of these dopants significantly overlapped with the valence band O 2p orbitals, which facilitated the transport of photo-generated charge carriers to the surface of the catalyst [1].

In earlier reported studies, N doping of TiO_2 is achieved by different methods such as treating anatase TiO_2 powders in an NH_3/Ar atmosphere [6], solution based methods like precipitation [7,8], sol-gel [9,10], solvothermal [11], hydro-thermal processes [12] and direct oxidation of the dopent containing titanium precursors at appropriate temperatures [13].

In this work nitrogen doped TiO_2 photocatalyst prepared via slow nucleation sol-gel method and crystal violet (CV, a kind of triarylmethane dye, Scheme 1.) chose as the target compound at photocatalytic studies.

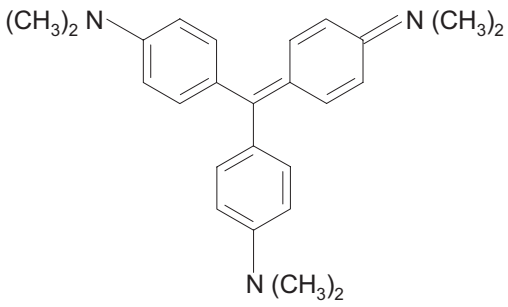

Scheme 1

2. EXPERIMENTAL

2. 1. Materials and Reagents

The chemicals used in this study were titanium tetrachloride ($TiCl_4$, 99.9%), Fluka, as a titanium precursor, urea (H_2NCONH_2, 98%), silver nitrate ($AgNO_3$), crystal violet ($C_{25}H_{30}N_3Cl$), hydrochloric acid and anhydrous ethanol (C_2H_5OH) from Merck. All reactant were used without further purification.

2. 2. Nitrogen Doped TiO_2 and Pure TiO_2 Preparation

Nitrogen doped TiO_2 and pure TiO_2 were prepared by the sol–gel method. For nitrogen doped TiO_2 preparation, 2 mL $TiCl_4$ was added to a 0.5 N hydrochloric acid solution under vigorous stirring in an ice water bath. Then 30 grams urea was added to reaction vessel. The mixture was stirred at 105 ˚C for 7 hours. After cooling at room temperature, the resulting solid was collected by filtration and washed with distilled water for several times. After washing, no Cl^- ion was detected by the reaction with 0.1 N $AgNO_3$ solution. The produced powder dried at 100 ˚C then calcined for 5 h at 450 ˚C.

The pure TiO_2 was prepared with the same method except no using hydrochloric acid and denoted as T photocatalyst.

2. 3. Characterization of the Products

Spectroscopic analyses of Nitrogen doped TiO_2 and pure TiO_2 samples were performed using UV–vis spectrophotometer (Shimadzu UV 2100) and Bruker, Eqinox 55 FT-IR spectrometer. Crystallite size, and phase identification of the product were characterized by X-ray diffraction (XRD) obtained on Philips X-pert diffractometer using a scan rate of 21/min and Cu Ka line (l=1.54056 A˚) radiation with working voltage and current of 40 kV and 40 mA, respectively. The morphology of the product was studied by scanning electron microscopy (SEM, Philips XL30). The (BET) specific surface area of the sample was determined through nitrogen adsorption (Micromeritics, Gemini 2370). TG–DSC was carried out using STA 150 Rhenometric Scientific unit. Measurements were taken with a heating rate of 10 ˚C/min from 25 to 800˚C in argon atmosphere.

2. 4. Photocatalytic Activity Determination

When photocatalyst nanoparticles adsorb light, it will generate electron–hole (e – h+) pairs which are able to initiate oxidation and reduction reactions to destroy the organic molecules. Photocatalytic activities of the prepared nitrogen doped TiO_2 and pure TiO_2 photocatalysts were evaluated by the degradation of crystal violet dye (CV) under visible light. For all photocatalytic experiments, a cylindrical glass was used as the reactor, which was filled with 300mL of aqueous suspension of CV (5 ppm) containing 1 g/L of photocatalysts. It was an open Pyrex glass tube with double walls, so that a jacket of water was cooling the reactor to constant temperature at 25±1 ˚C. An Osram lamp was used as the light source. Figure 1 shows the emission spectrum of Osram lamp. It was placed in a quartz vessel and immersed in center of photo reactor. Air was continuously bubbled into the solutions by an aquarium pump in order to provide a constant source of dissolved oxygen. Prior to irradiation, the suspension was magnetically stirred in the dark for approximately 30 min to ensure establishment of an adsorption/desorption equilibrium among the photocatalyst particles, CV, and atmospheric oxygen. During the course of visible light irradiation, a suspension of about 5mL was taken out after regular intervals, centrifuged, and then filtered through a Millipore

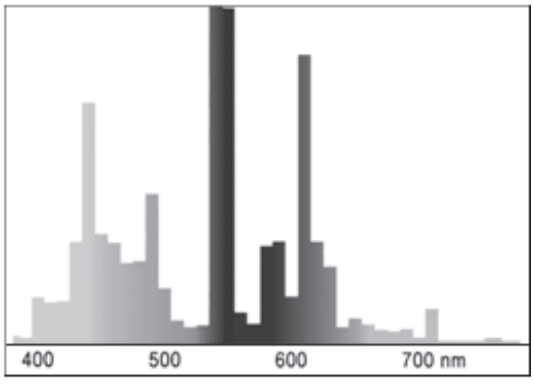

Fig. 1. Emission spectrum of Osram lamp.

filter. The filtrates were then studied by UV–vis spectroscopy.

3. RESULTS AND DISCUSSION

3. 1. Photocatalysts Characterization

The optical band gap (Eg) in a semiconductor was determined by plotting (ahv)1/m versus photon energy (hv) where a represents optical absorption coefficient and m represents the nature of transition. Now, m may have different values, such as 1/2, 2, 3/2 or 3 for allowed direct and indirect; and forbidden direct and indirect transitions, respectively [14, 15]. The plots of (ahv)1/2 for allowed indirect transitions of prepared pure TiO_2 (a) and nitrogen doped TiO_2 (b) samples dispersed in ethanol versus photon energy are shown in Figure 2 a and b. According to Figure 2 a, the extrapolated optical absorption gap of the pure TiO_2 is found to be 3.3 eV at room temperature. This is in agreement with the literature values for anatase TiO_2 [16, 17]. Similarly, as shown in Figure 2 b the optical absorption gap of nitrogen doped TiO_2 was found to be 2.8 eV. The visible light absorbance of nitrogen doped TiO_2 is of great significance for its practical application point of view.

The estimated indirect band gap of the prepared nitrogen doped TiO_2 reveals 0.5 eV red shift from value obtained for prepared pure TiO_2. The smaller band gap of the nitrogen doped TiO_2 in comparison to band gap value of pure TiO_2 is presumably due to the substitution of the lattice oxygen by nitrogen and formation of oxynitride center [18].

Figure. 3 shows the FTIR spectra of prepared nitrogen doped TiO_2 and pure TiO_2 samples. The broad peaks in the range 3000– 3400 cm^{-1} and 1630 cm^{-1} originated from surface adsorbed water and surface hydroxyl groups [19,20].The peak in between 1250 to 1500 cm^{-1} could be attributed to the entered nitrogen species in TiO_2 network [21, 22].

The crystalline structures of synthesized samples were investigated by XRD measurements. The XRD patterns obtained for nitrogen doped TiO_2 and pure TiO_2 samples are shown in Figure 4, curve a and b, respectively. The XRD patterns of the nitrogen doped sample can be assigned to pure anatase TiO_2 with

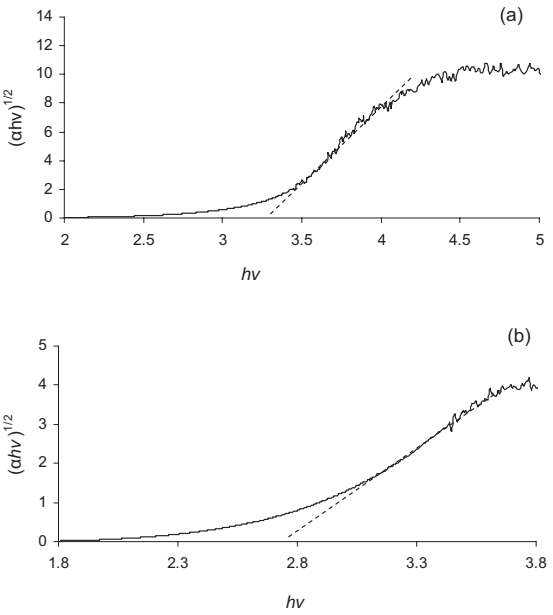

Fig. 2. $(ahv)^{1/2}$ as a function of photon energy for prepared pure TiO_2 (a) and nitrogen doped TiO_2 (b) samples dispersed in ethanol.

reflection peaks in (1 0 1), (0 0 4), (2 0 0), (1 0 5) and (2 1 1) crystal planes. However, the diffraction peaks for the pure TiO_2 sample can be ascribed to a mixed phase of rutile and anatase after calcination. The transition from anatase to rutile during the preparation of nitrogen doped TiO_2 was restrained by the doping of N in the lattice. This result is in agreement with the works reported by Yu and co-workers [23].

The average crystallite size of the synthesized nitrogen doped TiO_2 and pure TiO_2, calculated from the XRD data, according to Scherrer's equation, $D = 0.9\ \lambda / (\beta \cos\theta)$ where D is the average crystallite size (nm), λ is the applied X-ray wavelength (λ =1.5406 A˚), θ is the diffraction angle and β is a full-width at half the maximum of diffraction line observed in radians. According to Scherrer's equation, the average crystallite sizes of pure TiO_2 and nitrogen doped TiO_2 samples are 17.43 and 24.07 nm,

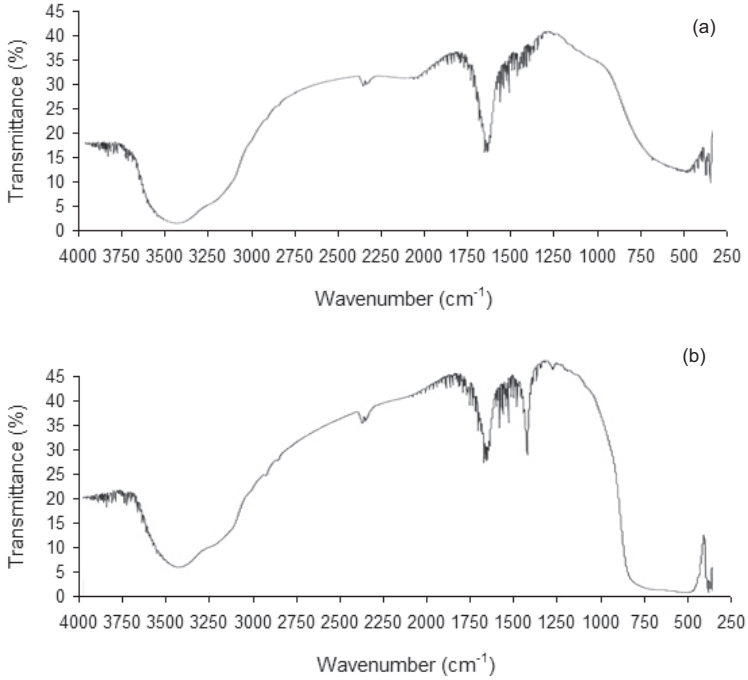

Fig. 3. FTIR spectra of prepared pure TiO_2 (a) and nitrogen doped TiO_2 (b) samples.

respectively. According to the quantum size effect theory, the band-gap of the semiconductor is very sensitive to the nanoparticle size, the smaller the semiconductor particle size, the wider the band-gap.

Figure 5 shows SEM images of prepared pure TiO_2 and nitrogen doped TiO_2 nanoparticles. These images confirm that both of samples

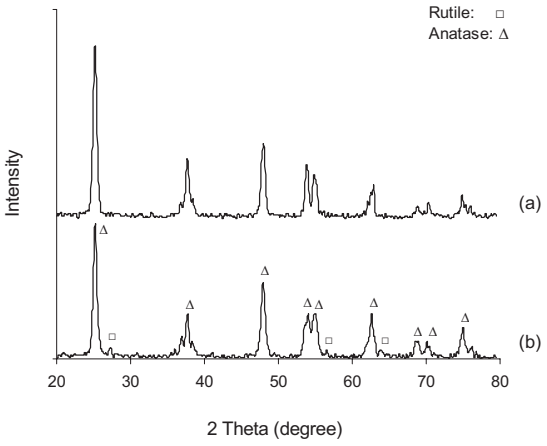

Fig. 4. XRD patterns of prepared nitrogen doped TiO_2 (a) and pure TiO_2 (b).

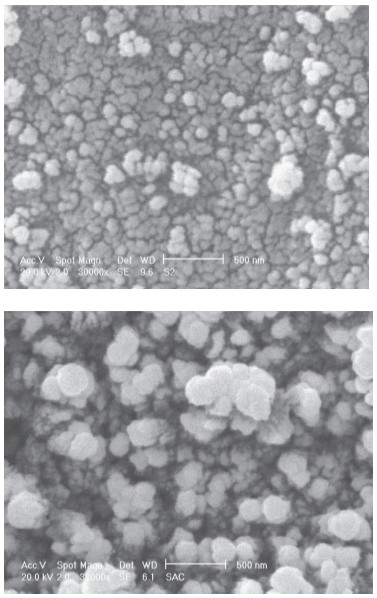

Fig. 5. SEM images of prepared pure TiO_2 (a) and nitrogen doped TiO_2 (b) nanoparticles.

exhibit the form of spherical particle and are to some extend agglomerated.

Figure. 6 shows the N_2-adsorption isotherms as a function of P/P_0. The (BET) specific surface areas of the samples were determined through their nitrogen adsorption isotherms. According to Figure 6, both of isotherms are of type IV which proves the presence of mesopores within the synthesized samples [24, 25]. The BET surface areas of pure TiO_2 and nitrogen doped TiO_2 nanoparticles are 43.79 and 54.55 m2g-1, respectively deduced from the plots.

Differential scanning calorimetry and thermogravimetric curves of pure TiO_2 and nitrogen doped TiO_2 samples are shown in Figure 7.

For pure TiO_2 sample, the decrease in weight, up to 296 ˚C is attributed to desorption of the physisorbed water and organic residues (confirmed by three endothermic peaks on the DSC curve at about 110, 236 and 296 ˚C). According to TG analysis, a large number weight loss, 44.28%, is observed up to 296 ˚C as a result of remove of physisorbed water and organic residues. After that, the weak thermal effect at 350-500 ˚C is accompanied by obvious exothermic peak at around 460 ˚C in DSC curve which confirms the crystallization of the amorphous phase to anatase. Above 460 ˚C, the change in weight is very small.

For nitrogen doped TiO_2 sample, removal of physisorbed water and organic residues tack place up to 220 ˚C which is accompanied by two significant endothermic peaks in DSC curve. TG analysis shows that the weight loss at 220 ˚C is 19.03%. The weight loss as a result of physisorbed water and organic residues at nitrogen doped TiO_2 sample is smaller than pure TiO_2 sample. Furthermore, a diffuse exotherm at around 350 ˚C in DSC curve which confirms the crystallization of the amorphous phase to anatase is not accompanied with large weight loss in the temperature range of 300-500 ˚C. It can be described as remaining of some nitrogen spices in the nitrogen doped TiO_2 network during heat treatment.

3. 2. Formation Mechanism of Nitrogen Doped TiO_2

The reaction was started by producing $TiO(OH)_2$ as a result of slow hydrolyze of $TiCl_4$ in an acidic solution. After that, PH slowly increased by gradually decomposition of added urea. The finding is consistent with Kuroda et al.

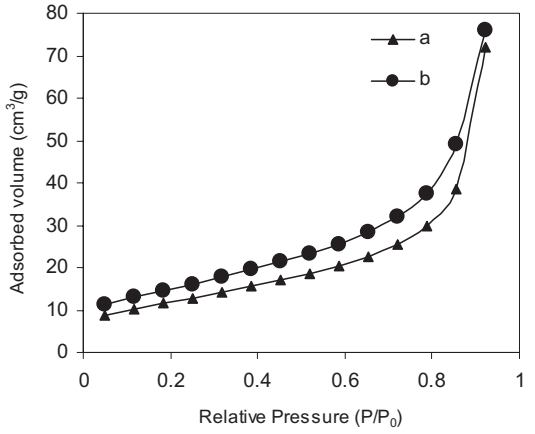

Fig. 6. N_2-adsorption isotherms of prepared pure TiO_2 (a) and nitrogen doped TiO_2 (b) samples.

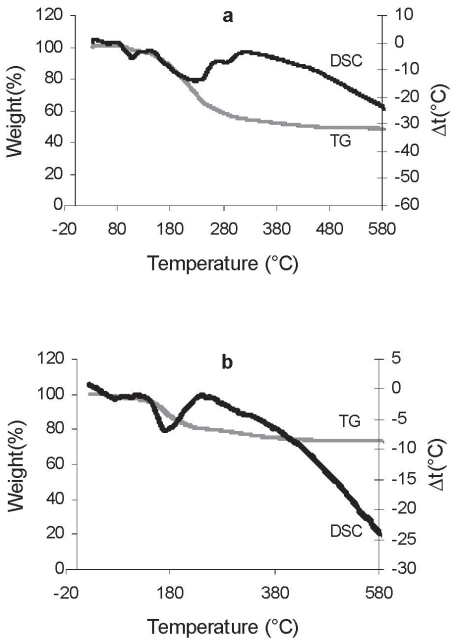

Fig. 7. TG-DSC curves of prepared pure TiO_2 (a) and nitrogen doped TiO_2 (b) samples.

approach which showed that NH_2CONH_2 decomposed by heat treatment into $OH^- + NH^{4+} + CO_2$ [26]. The prepared $TiO(OH)_2$ acts as a strong Lewis acid site and then adsorb the ammonia, water and other intermediate product of hydrolysis of urea [26]. Then the adsorbed species are transformed in to NH_2 and OH after heat treatment and finally nitrogen is incorporated in to TiO_2 lattice by dehydration and condensation reaction to form anatase TiO_2−xNx.

3. 3. Photocatalytic Activity

Figure 8 shows the efficiency of photodegradation (X) of the nitrogen doped TiO_2 in comparison to pure TiO_2 photocatalyst for the removal of crystal violet as a function of time at $\lambda = 587$ nm. Here $X = (C_0\text{-}C)/C_0$, where C_0 is the initial concentration of dye, and C is the concentration of dye at time T. As shown in Figure 8, nitrogen doped TiO_2 has high efficiency of 78% in crystal violet decolorization in 120 minutes but pure TiO_2 shows no significant photocatalytic efficiency under visible light.

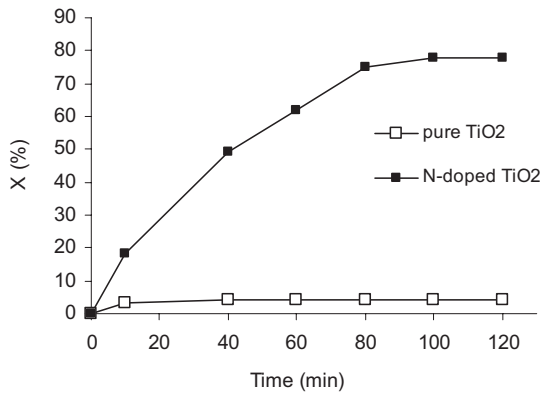

Fig. 8. The degree of photocatalytic degradation (X) as a function of irradiation time at 587 nm for pure TiO_2 (□) and Nitrogen doped TiO_2 (■).

4. CONCLUSION

Yellow-colored nitrogen doped TiO_2 powder was synthesized by a simple sol-gel acid catalyst reaction. Here the synthesis procedure deals with controlled precipitation and slow nucleation and growth of nitrogen doped TiO_2 nanoparticles. The preparation of nitrogen doped TiO_2 resulting in a desired band gap narrowing and an enhancement in the phtocatalytic activity under visible light.

5. ACKNOWLEDGMENTS

Support by Nuclear Science and Technology Research Institute of Atomic Energy Organization of Iran, Tarbiat Modares University and Iran National Science Foundation (INSF) is greatly appreciated.

REFRENCES

1. Janitabar Darzi, S., Mahjoub, A. R., Nilchi, A. R., Rasouli Garmarodi, S., "Heattretment effects on non-thermal sol-gel drived mesoporous TiO_2/SiO_2", Iran. J. Mater. Sci. Eng., 2011, 8, 20-26.
2. Komai, Y., Okitsu, K., Nishimura, R., Ohtsu, N., Miyamoto, G., Furuhara, T., Semboshi, S., Mizukoshi, Y., Masahashi, N., "Visible light response of nitrogen and sulfur co-doped TiO_2 photocatalysts fabricated by anodic oxidation", Catal. Today, 2011, 164, 399-403.
3. Safaei-Naeini, Y., Aminzare, M., Golestani-Fard, F., Khorasanizadeh, F., Salahi, E., "Suspension Stability of titania nanoparticles studied by UV-VIS spectroscopy method", Iran. J. Mater. Sci. Eng., 2012, 9, 62-68.
4. Hamadanian, M., Reisi-Vanani, A., Majedi, A., "Preparation and characterization of S-doped TiO_2 nanoparticles, effect of calcination temperature and evaluation of photocatalytic activity", Materials Chemistry and Physics 2009, 116, 376-382.
5. Liu, S., Chen, X., "A visible light response TiO_2 photocatalyst realized by cationic S-doping and its application for phenol degradation", J. Hazard.Mater. 2008, 152, 48–55.
6. Irie, H., Watanabe, Y., Hashimoto, K., "Nitrogen- concentration dependence on photocatalytic activity of TiO_2-xNx powders", J. Phys. Chem. B, 2003, 107, 5483–5486.
7. Yu, J. G., Zou, M. H., Cheng, B., Zhao, X. J., "Prepara-tion, characterization and

photocatalytic activity of in situ N, S-codoped TiO_2 powders," J. Molec. Catal. A: Chem., 2005, 246, 176–184.

8. Wang, Y. Q., Yu, X. J., Sun, D. Z., "Synthesis, characterization, and photocatalytic activity of TiO_2−xNx nano- catalysts," J. Hazard. Mater., 2006, 144, 328–333.
9. Gole J. L., Stout, J. D., Burda, C., Lou, Y., Chen, X., "Highly efficient formation of visible light tunable TiO_2-xNx photocatalysts and their transformation at the nanoscale," Journal of Physical Chemistry B., 2003, 108, 1230–1240.
10. Burda, C., Lou, Y., Chen, X., Samia, A. C. S., Stout, J., Gole, J. L., "Enhanced nitrogen doping in TiO_2 nanoparti-cles," Nano Lett., 2003, 3, 1049–1051.
11. Chi, B., Zhao, L., Jin, T., "One-step template-free route for synthesis of mesoporous N-doped titania spheres," J. Phys. Chem. C, 2007, 111, 6189– 6193.
12. Bao, X. W., Yan, S. S., Chen, F., Zhang , J. L., "Preparation of TiO_2 photocatalyst by hydrothermal method from aqueous peroxotitanium acid gel," Mater. Lett., 2004, 59, 412-415.
13. Morikawa, T., Asahi, R., Ohwaki, T., Aoki, K., Taga, Y., "Band-gap narrowing of titanium dioxide by nitrogen doping" Japan Journal of Applied Physics, 2001, 40, 561–563.
14. Bhattacharyya, D., Chaudhuri, S., Pal, A. K., "Bandgap and optical transitions in thin films from reflectance measurements", Vacuum, 1992, 43, 313-316.
15. Linsebigler, A. L., Lu, G. Q., Yates J. T., "Photocatalysis on TiO_2 Surfaces: Principles, Mechanisms, and Selected Results",Chem. Rev. 1995, 95, 735-758.
16. Tang, H., Prasad, K., Sanjines, R., Schmid, P. E., Levy, F., "Electrical and optical properties of TiO_2 anatase thin films", J. Appl. Phys., 1994, 75, 2042-2047.
17. Fox, M. A., Dulay, M. T., "Heterogeneous photocatalysis", Chem. Rev. 1993, 93, 341–357.
18. Parida, K.M.; Naik, B., "Synthesis of mesoporous TiO_2−xNx spheres by template free homogeneous co-precipitation method and their photo-catalytic activity under visible light illumination", J.Colloid. Interf. Sci. 2009, 333, 269-276
19. Ding, Z., Lu, G. Q., Greenfield, P. F., "role of the Crystallite Phase of TiO_2 in Heterogeneous Photocatalysis for Phenol Oxidation in Water", J. Phys. Chem. B. 2000, 104, 4815-4820.
20. Machado, N., Santana, V. S., " Influence of thermal treatment on the structure and photocatalytic activity of TiO_2 P25", Catal. Today, 2005, 107-108, 595-601.
21. Shanmugasundaram, S., Marcin, J., Kisch, H.," Visible Light Activity and Photoelectrochemical Properties of Nitrogen-Doped TiO_2", J. Phys. Chem. B., 2004, 108, 19384-19387.
22. Li, H., Li, J., Hou, Y.," Highly Active TiO2N Photocatalysts Prepared by Treating TiO_2 Precursors in NH_3/Ethanol Fluid under Supercritical Conditions", J. Phys. Chem. B., 2006, 110, 1559-1565.
23. Wang, Y. Q., Yu, X. J., Sun, D. Z., "Synthesis, characterization, and photocatalytic activity of TiO_2-x Nx nanocatalyst", J. Hazard. Mater.,2007, 144, 328-333.
24. Janitabar Darzi, S., Mahjoub, A. R., Nilchi, A.,"Synthesis of Spongelike Mesoporous Anatase and its Photocatalytic Properties", Iran. J. Chem. Chem. Eng , 2010, 29, 37-42.
25. Kruk, M., Jaroniec, M., "Gas Adsorption Characterization of Ordered Organic-Inorganic Nanocomposite Materials", Chem. Mater. 2001, 13, 3169-3183.
26. Kuroda, Y.; Mori, T.; Yagi, K.; Makihata, Kawahara, Y.; Nagao, M.; Kittaka, S.; "Preparation of Visible-Light-Responsive TiO_2-xNx Photocatalyst by a Sol−Gel Method: Analysis of the Active Center on TiO_2 that Reacts with NH3", Langmuir, 2005, 21, 8026-8034.